Electronic Supplementary Information (ESI†)

Modulation of Glyceraldehyde-3-phosphate dehydrogenase Activity by Surface Functionalized Quantum Dots

Srabanti Ghosh*[a], Manju Ray[b], Mahua Rani Das[c], Adrita Chakrabarti[a], Ali Hossain Khan[a], D. D. Sarma[d], and Somobrata Acharya*[a]

[a]Centre for Advanced Materials, Indian Association for the Cultivation of Science, Kolkata-700032, India. [b]Division of Molecular Medicine, Bose Institute, Kolkata 700 054, India. [c]Biological Chemistry, Indian Association for the Cultivation of Science, Kolkata-700032, India. [d]Solid State and Structural Chemistry Unit & Centre for Condensed Matter Theory Indian Institute of Science, Bangalore 560012, India

*Corresponding Author, E-mail: ghosh.srabanti@gmail.com, camsa2@iacs.res.in

Determination of the average particle size and concentration:

CdS and CdTe QDs were synthesized colloidal method as reported earlier with trivial modification.[1] QDs exhibit a blue shift in the absorption spectra as the size is reduced below the characteristic Bohr exciton diameter of the bulk material.[2,3] The band gap (E_g) was calculated from absorption onset (λ_{onset}) in the UV-Vis absorption spectra of each nanoparticle solution using the relation, $E_g = hc/\lambda_{onset}$, where h is the Planck's constant and c is the speed of light. The average size of QDs (d) was obtained using the correlation of band gap shift ($\Delta E_g = E_{g(QDs)} - E_{g(bulk)}$), and particle size deduced by tight-binding approximation.[4]

$$\Delta E_g = a_1 e^{-d/b_1} + a_2 e^{-d/b_2} \qquad (1)$$

The values of the parameters for CdS QDs are a_1=2.83, b_1=8.22, a_2=1.96 and b_2=18.07 and for CdTe QDs are a_1=5.77, b_1=8.45, a_2=1.33 and b_2=43.73. The size determined from the respective absorption onset is in agreement with average size determined from Transmission Electron Microscopy (TEM, Fig. S1a and S1b).

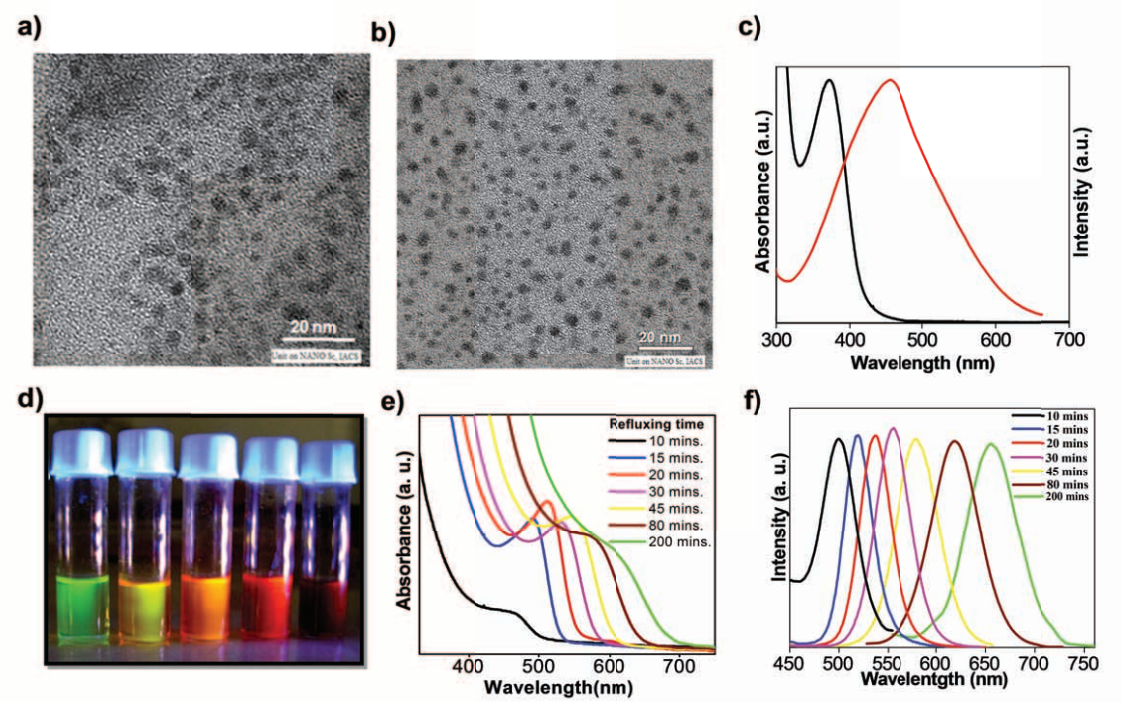

Fig.S1 TEM images of a) CdS_{MPA} QDs and b) CdS_{NAC} QDs. TEM reveals QDs has an average particle size of 3 ± 1 nm, which is in agreement with the size determined from the respective absorption onset. c) UV-vis absorption (black line) and photoluminescence (red line) spectra of typical CdS_{NAC}. The absorption peak of CdS QDs appears at ~ 370 nm while the corresponding photoluminescence shows a fair overlapping with the absorption peak. d) Size dependent photoluminescence colour of the $CdTe_{NAC}$ QDs (λ_{ex} = 390 nm). The graph shows size dependent optical properties of quantum dots where e) represents UV-Vis absorption and f) represent photoluminescence spectra of $CdTe_{NAC}$ at different refluxing time. The functionalized biocompatible QDs show size dependent luminescence properties spanning from 480 nm to 680 nm with quantum yield ~25-45% suggesting suitability for fluorescence based sensing and detection tests.

The concentrations of QDs were calculated using the correlation of the molar extinction coefficient with particle diameter and absorbance values observed for the respective QD-solutions.[5] A clearly resolved absorption maximum of the first electronic transition of CdTe QDs appears at λ_{max} ~ 460 nm in 10-12 min after beginning of reflux, corresponding to the smallest CdTe QDs (~2 nm) which shifted to longer wavelengths in the course of heating (Fig. S1e). The size of the CdTe QDs is controlled by the duration of reflux and can easily be monitored by absorption and photoluminescence spectra as shown in Fig. S1e and Fig. S1f. The duration of the heat treatment necessary to reach a certain particle size depends on the nature of the capping

agent. The quantum yield was measured at room temperature by comparing with the fluorescence emission of quinine sulfate. The functionalized biocompatible QDs show size dependent luminescence properties spanning from 480 nm to 680 nm with quantum yield ~25-45% suggesting suitability for fluorescence based sensing and detection tests.[6-8]

GAPDH Assay:

GAPDH was routinely assayed in triethanolamine-HCl buffer pH 8.5 based on a modification of the method developed by Krebs.[9,10] To monitor the reaction, the increase in absorbance at 340 nm due to the formation of NADH from NAD was noted at 30 seconds intervals as shown in Fig. S2. The protein concentration was estimated with BSA as standard following Lowry method.[11] Assays were normally conducted in triplicate.

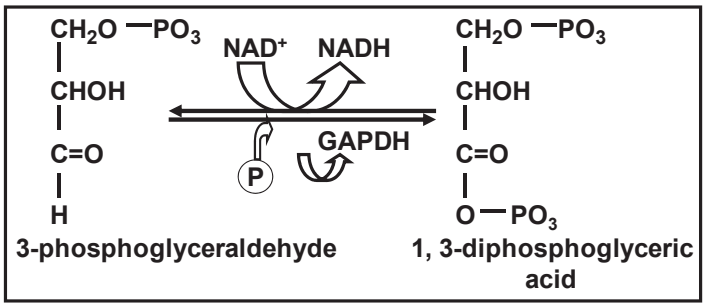

Fig.S2 Biochemical reaction involved in the GAPDH enzyme assay. The GAPDH catalyzed the oxidative phosphorylation of D-glyceraldehyde-3-phosphate (GAP) to 1,3-diphosphoglycerate (1,3DPGA) in presence of NAD^+, inorganic phosphate and the formation of NADH was monitored at 340 nm.

Development of tumour:

Sarcoma tissue was developed in left hind leg of mice by intramuscular injection of 3-methyl-cholanthrene. The carcinogen was dissolved in olive oil by placing it in warm water-bath and 0.1 mL of olive oil containing 0.2 mg of the carcinogen was injected into each mouse thrice with one-week interval. After 12-14 weeks full-grown tumour was developed (Fig.S3). The malignancy was confirmed by histological examination where differtiated muscle cells are conspicuously visible in normal mouse muscle and highly differentiated sarcoma tissue is being observed, where tumour was developed by 3-methyl-cholanthrene (Fig.S4).

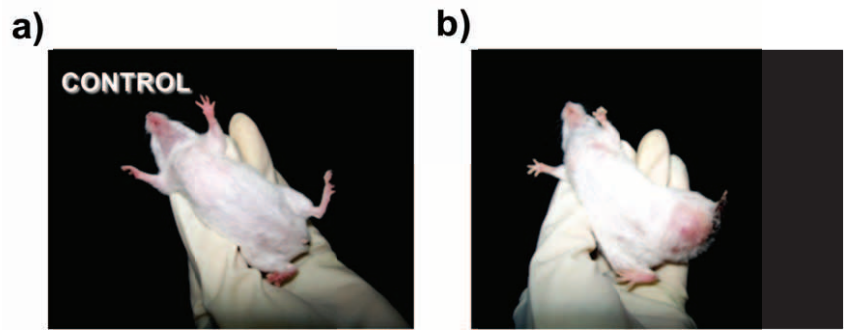

Fig.S3 Photographs represents a) normal mice and b) tumour generated (in left hind leg) mice.

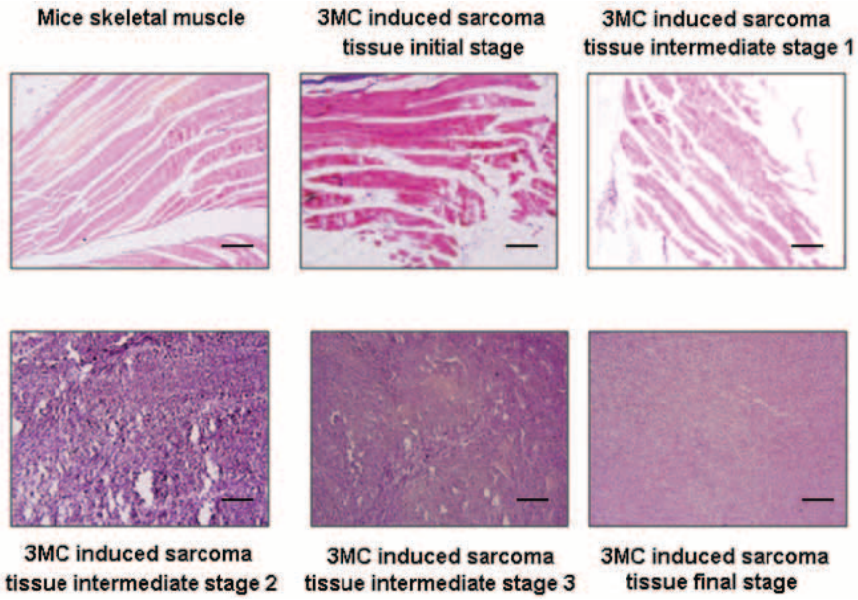

Fig.S4 Histological examination of mice skeletal muscle with 3MC induced sarcoma tissue at different stages, Initial stage, Intermediate stages with progression of malignancy and full grown tumor. The stain used was eosin and hematoxylin.

Purification of GAPDH from normal muscle, sarcoma tissue and ehrlich ascites carcinoma (EAC) cells.

15 gm of either normal mice muscle or sarcoma tissue or carcinoma cells (Fig. S5) was homogenized in an Omni GLH International homogenizer with four volumes of 50 mM triethanolamine-HCl buffer, pH 7.4 containing 10 mM EDTA and 10 mM β-mercaptoethanol. The tissue and the buffer were pre-cooled and all operations were carried out at 0-4°C. From the homogenate, GAPDH was purified by gel filtration and ion exchange chromatography. The enzyme fractions after DEAE-sephacell column step were purified 28 and 96 fold for normal

muscle and sarcoma tissues respectively. The specific activities of GAPDH at this stage were 112 for normal muscle and 313 for sarcoma tissue.

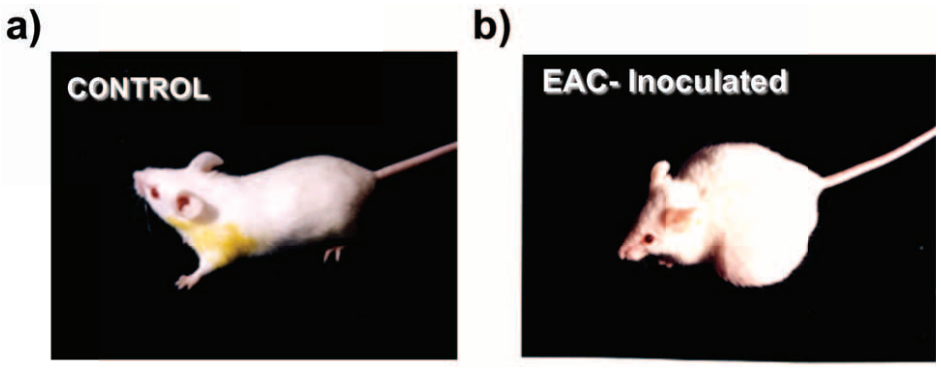

Fig.S5 a) Normal mice as control and b) EAC cells maintained in the peritoneal cavity of the mice.

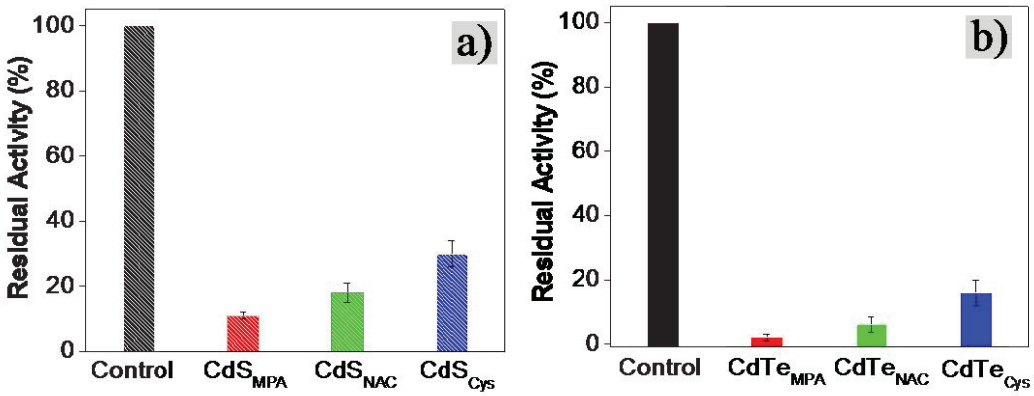

Fig.S6 a) Effect of CdS quantum dots with different thiol groups; 3-mercaptopropionic acid (MPA, red bar), N-acetyl L-cysteine (NAC, green bar) and cysteine hydrochloride (Cys, blue bar) on the activity of GAPDH. Rabbit muscle GAPDH in absence of CdS QDs as control (black bar) is shown. The inhibition of GAPDH at maximum concentration of 60 nM follow the trend as CdS_{Cys}<CdS_{NAC}<$CdS_{MPA.}$ The MPA coated QDs are found to be the most efficient inhibitors owing to the presence of electrostatic interaction between the carboxylate end groups of QDs and cationic residues in the periphery of active site of GAPDH. b) Effect of CdTe quantum dots with different thiol groups; MPA (red bar), NAC (green bar) and Cys (blue bar) on the activity of GAPDH. Rabbit muscle GAPDH in absence of CdS QDs as control (black bar) is shown. The inhibition of GAPDH at maximum concentration of 60 nM follow the trend as $CdTe_{Cys}$<$CdTe_{NAC}$ <$CdTe_{MPA.}$ The MPA coated QDs are found to be the most efficient inhibitors owing to the presence of electrostatic interaction between the carboxylate end groups of QDs and cationic residues in the periphery of active site of GAPDH.

Quantum dots	Zeta potential (mV)
CdS_{MPA}	-32
CdS_{NAC}	-18
CdS_{Cys}	-5

Table S1. Average zeta potentials of CdS QDs capped with three different thiols; MPA, NAC and Cys.

The CdS_{MPA} or $CdTe_{MPA}$ are the most efficient inhibitors owing to the presence of electrostatic interaction between the carboxylate end groups of CdS/CdTe QDs and cationic residues in the periphery of active site of GAPDH. The CdS_{MPA} having larger numbers of the surface carboxylate (-COOH) groups are proposed to contribute maximum electrostatic interactions between GAPDH and QDs with high negative surface charge density as reflected in zeta potential measurements (Fig.S6 and Table S1). However, CdS_{Cys} having lower surface charge containing both carboxylate (COOH) and amine (NH_2) groups interact with lesser number of enzyme molecules in comparison to CdS_{MPA}.

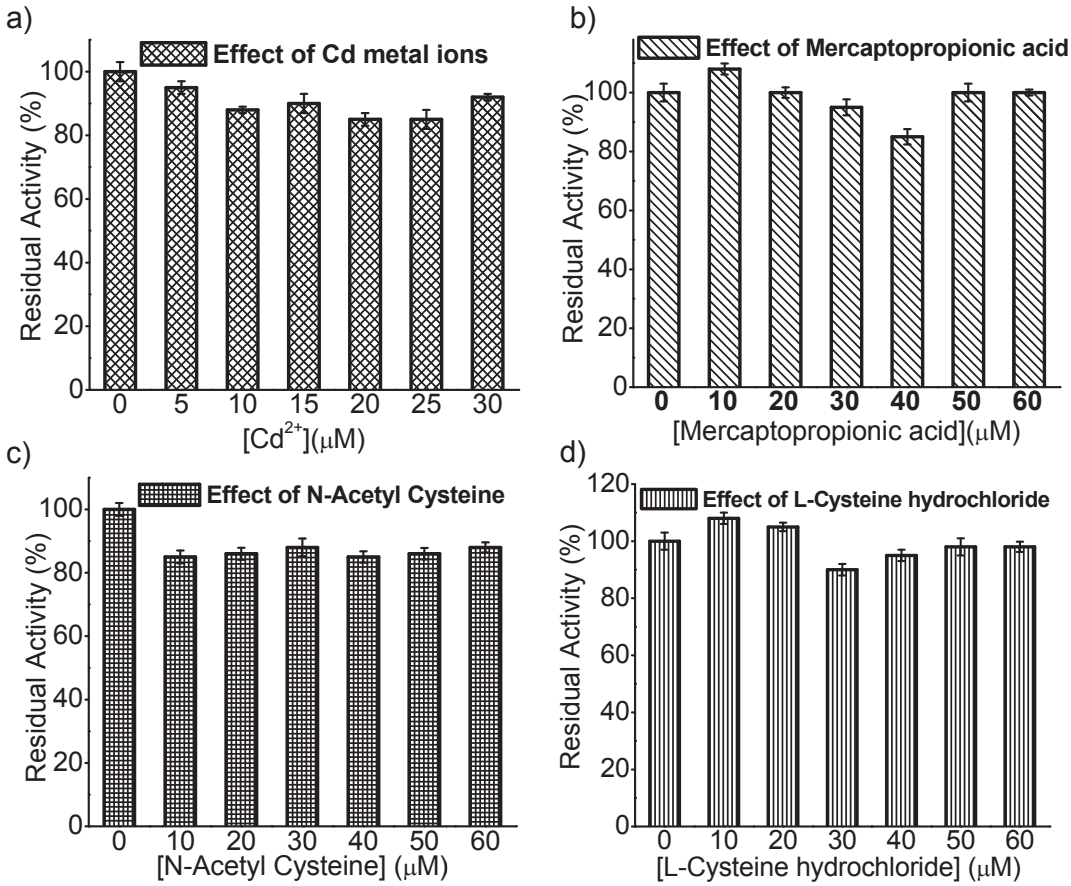

Fig.S7 Effect of a) cadmium metal ions ( ), b) 3-mercaptopropionic acid ( ), c) N-acetyl L-cysteine ( ) and d) L-cysteine hydrochloride ( ) on the activity of R-GAPDH. The graph shows none of capping agents and cadmium metal ions shows inhibition of enzyme activity suggesting the electrostatic interaction originated from the QDs resulting in GAPDH inhibition.

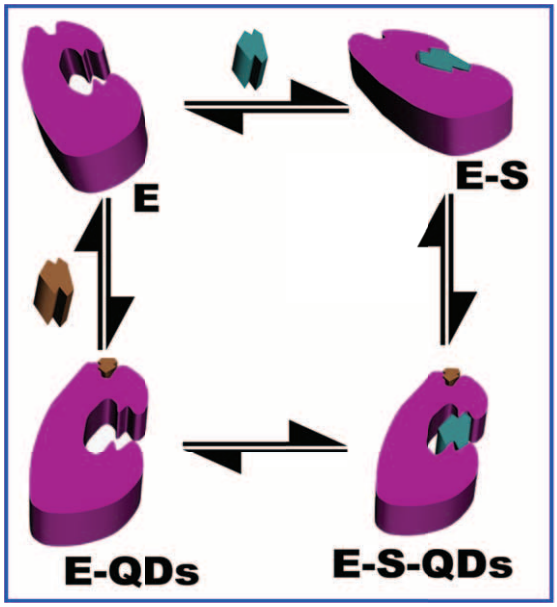

Fig.S8 Mechanistic representationsof enzyme inhibition via noncompetitive pathway.

According to the Michaelis–Menten treatment of a reversible inhibition, non-competitive inhibitor does not change K_m (i.e., it does not affect substrate binding) but decreases V_{max} (i.e., inhibitor binding hampers catalysis).[12] The effects of different types of reversible enzyme inhibitors on enzymatic activity can be visualized using graphical representations of the Michaelis–Menten equation, such as Lineweaver–Burk plot. The V_{max} is determined by carrying out experiments to generate a Line weaver–Burk plot as defined by

$$\frac{1}{V} = \frac{K_m}{V_{max}} \frac{1}{[S]} + \frac{1}{V_{max}} \tag{2}$$

$$V = V_{max} \frac{[S]}{[S] + K_m} \tag{3}$$

A plot of 1/V versus 1/[S] should be linear, and V_{max} can be determined from the inverse of the intercept. The equation used for the Dixon plot[13] to determine the K_i value of inhibitor is

$$\frac{1}{V} = \left(\frac{K_m}{V_{max} K_i} \right) [I] + \frac{1}{V_{max}} \left(1 + \frac{K_m}{[S]} \right) \tag{4}$$

where v is the velocity of the reaction at inhibitor concentration, [I], V_{max} is the maximum velocity of the enzyme at the concentration of substrate in absence of inhibitor, [S] is the

concentration of substrate, K_m is the Michaelis constant, and K_i is the equilibrium constant of the inhibitor binding to the enzyme. A plot of 1/V versus [I] should be linear, and K_i can be determined from the slope and intercept of the line and V_{max}.

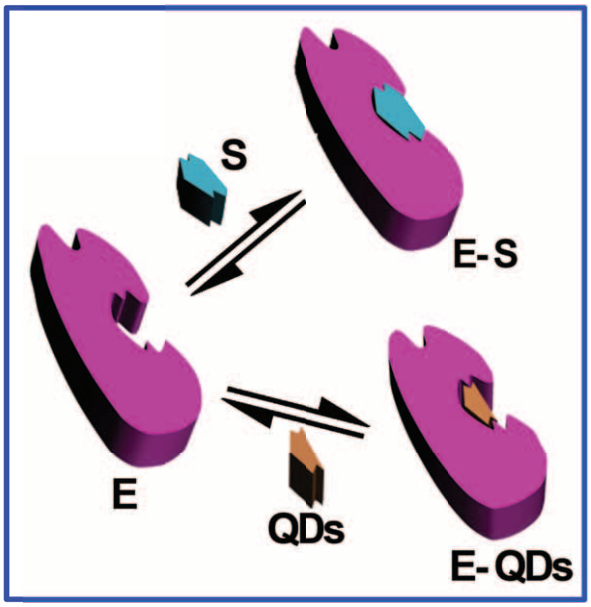

Fig.S9 Mechanistic representation of enzyme inhibition via competitive pathway.

In competitive inhibition, inhibitors can bind to enzyme (E), but not to enzyme-substrate complex (ES). Hence, competitive inhibitors increases K_m as the inhibitor interferes with substrate binding but does not affect V_{max} (the inhibitor does not hamper catalysis in ES because it cannot bind to ES).[12] Hence, according to the Michaelis–Menten treatment of a reversible inhibition, V_{max} is unaffected by the inhibitor, but the apparent K_m will vary with inhibitor concentration.

In mixed inhibition, inhibitors can bind to both E and ES, but their affinities for these two forms of the enzyme are different. Thus, mixed-type inhibitors interfere with substrate binding (increase K_m) and hamper catalysis in the ES complex (decrease V_{max}). This type of inhibition can be reduced, but not overcome by increasing concentrations of substrate. The mixed type inhibition generally happens from an allosteric effect where the inhibitor binds to a different site on an enzyme. Hence, inhibitor binding to this allosteric site affects the conformation of three-dimensional structure of the enzyme so that the affinity of the substrate for the active site is reduced.

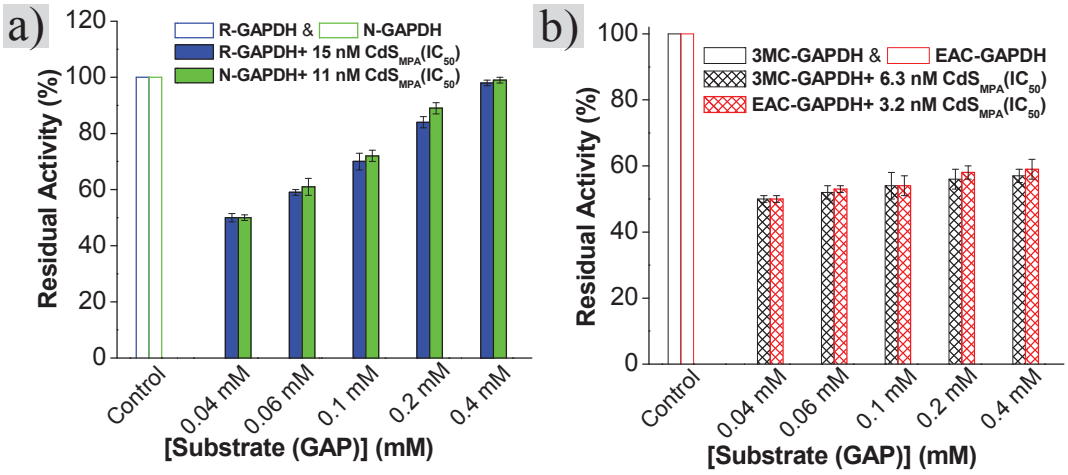

Fig.S10. a) The inhibition of R-GAPDG and N-GAPDH by CdS_{MPA} at IC_{50} value in presence of various GAP concentrations. Control represents R-GAPDG (black bar) and N-GAPDH (red bar) in absence of CdS_{MPA}. The graph shows the activities N-GAPDG and R-GAPDH are reversibly regained activity with increasing concentration of GAP suggesting QDs induced reversible inhibition. b) The inhibition of 3-MC and EAC GAPDH by CdS_{MPA} at IC_{50} value in presence of various GAP concentrations. Control represents 3-MC (black bar) and EAC (red bar) GAPDH in absence of CdS_{MPA}. The graph demonstrates that the activities EAC and 3-MC GAPDH are not recovered with increasing concentration of GAP suggesting QDs induced irreversible inhibition.

We have tested the inhibition of both normal and malignant GAPDH in presence of CdS_{MPA} at IC_{50} values with increasing concentration of substrate (GAP). In case of N-GAPDH and R-GAPDH, 50% inhibition of activity reversibly regained activity with increasing concentration of GAP (Fig.S10a). However, for EAC and 3-MC GAPDH, activities are not recovered suggesting a QDs induced irreversible inhibition (Fig.S10b).The differential mode of interaction may be attributed due to the presence of different amino acid residues at the active site of the enzyme molecule.

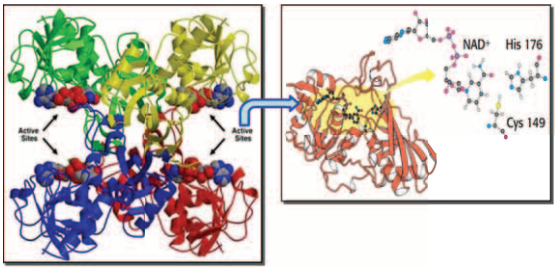

Fig.S11 Molecular structure of Rabbit GAPDH from protein data bank.

Gel electrophoresis for molecular weight determination: For determination of molecular weight of GAPDH of EAC cells, sarcoma tissue and normal muscle the samples were gel filtered on a Sephacryl S-200 column using cytochrome *c*, ovalbumin, BSA, and alcohol dehydrogenase as reference marker proteins.

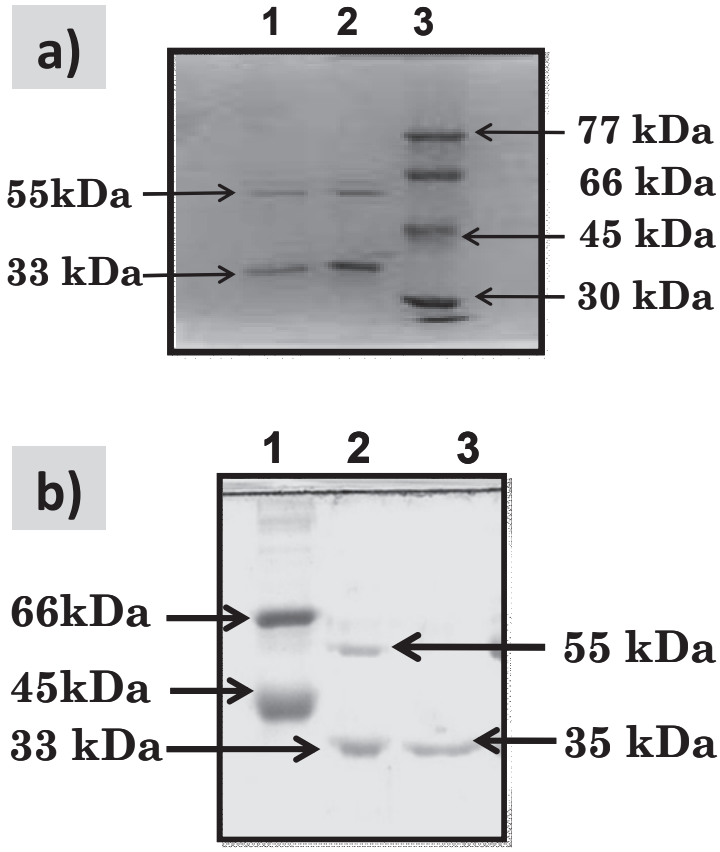

Fig.S12 a) SDS-PAGE of purified GAPDH from Ehrlich Ascites Carcinoma (EAC) cells. 1 and 2 represents EAC GAPDH (6 µg and 8 µg protein) and Lane 3 molecular weight marker.The SDS-PAGE suggests EAC GAPDH is a heterodimer molecule with two unequal subunits of molecular weight 55 kDa and 33 kDa. b) SDS-PAGE of GAPDH purified from normal mouse muscle and sarcoma tissue. Lanes 1-3 represent BSA (66 kDa) plus Ovalbumin (45 kDa), sarcoma tissue GAPDH (8µg protein), normal muscle GAPDH (6µg protein) respectively. The SDS-PAGE shows the N-GAPDH is a homotetramer of molecular weight 140 kDa, with subunit molecular weight 35 kDa. In contrasts, 3MC-GAPDH is altered with two subunits of molecular weight 55 kDa and 33 kDa.

The subunit molecular weight has been found out in SDS-polyacrylamide gel electrophoresis (Fig.S12a-b). The SDS-PAGE illustrates normal mouse muscle has a single band corresponding to molecular mass 35 ± 1 kDa, which is similar to that of normal mammalian muscle enzyme such as rabbit muscle GAPDH.[14] In contrast, GAPDH of both EAC cells and sarcoma tissues

showed two unequal subunits of 54 ± 2 and 33 ± 1 kDa which is consistent with earlier report.[15] The molecular weight of GAPDH purified from various normal mammalian sources is 140 kDa. This enzyme contains four identical subunits of 35 kDa. But, it is interesting to note that EAC-GAPDG and 3 MC-GAPDH enzymes are a heterodimer of molecular mass 87 ± 3 kDa. This indicates that the molecular mass and subunits of malignant cell enzyme may be altered in malignant cells due to the possible alternations in the primary or other structures of the protein molecule. The partial sequence of 33 kDa and 55 kDa subunit of sarcoma GAPDH is different in comparison to the partial sequence of other four subunit/proteins (Table S2).

Protein	Reference	Partial N-terminal sequence
33 KDa EAC GAPDH	Ghosh et al. Eur. J. Biochem. **2001**, *268*, 6037–6044	VIVGVNGKGRIGSLVSDDLI
55 KDa EAC GAPDH	Ghosh et al. Eur. J. Biochem. **2001**, *268*, 6037–6044	KDLQQWATWTDETWTL
33 KDa Sarcoma GAPDH	Patra et al. Biochem. (Moscow), **2009**, *74*, 717–721	VNVGVNGFGRIGGLV VAA
55 KDa Sarcoma GAPDH	Patra et al. Biochem. (Moscow), **2009**, *74*, 717–721	SKVGVNGFGRIKRLVTVAA
GAPDH (mouse)	NCBI Protein Database Acc. No. AAH85315	MVKVGVNGFGRIGRLVTRAA
GAPDH (rabbit)	NCBI Protein Database Acc. No. P46406	MVKVGVNGFGRIGRLVTRAA
Tumor protein, transcriptionally controlled	NCBI Protein Database Acc. No. XP-00148705	MVKVN GFGRIRRLVTRAA

Table S2. Partial sequence of subunits of EAC and sarcoma GAPDH.

Mitochondrial respiration	ADP stimulation rate (nmol/ml/mg)	Rate after addition of 50 µg CdS_{MPA} (nmol/ml/mg)	% Inhibition
Sarcoma	14.3±2.2	8.5±2.3	40%
EAC	12.6 ±2.3	5.8±1.1	54%

Table S3. Effect of CdS_{MPA} on respiration of sarcoma tissue and EAC mitochondria at 25°C.

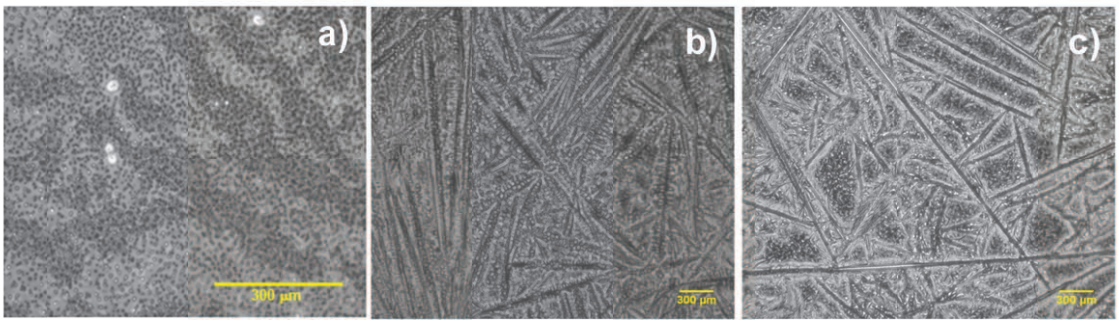

Fig.S13 Bright field image of a) quantum dots, b) R-GAPDH in absence CdS_{NAC} and c) presence of CdS_{NAC} at 10X.

Supplementary Information References:

1. A. Priyam, S. Ghosh, S. C. Bhattacharya and A. Saha, *J. Colloid Interface Sci*., 2009, **331**, 195 -201.
2. X. Michalet, F. F. Pinaud, L. A. Bentolila, J. M. Tsay, S. Doose, J. J. Li, G. Sundaresan, A. M. Wu, S. S. Gambhir and S. Weiss, *Science,* 2005, **307**, 538-544.
3. M. Bruchez Jr, M. Moronne, P. Gin, S. Weiss and A. P. Alivisators, *Science,* 1998, **281**, 2013-2016.
4. S. Sapra and D. D. Sarma, *Phys. Rev. B,* 2004, **69**, 125304-125310.
5. W. W. Yu, L. Qu, W. Guo and X. Peng, *Chem. Mater.,* 2003**, 15**, 2854-2860.
6. S. Ghosh, A. Priyam, S. C. Bhattacharya and A. Saha, *J. Fluoresc.,* 2009, **19,** 723-731.
7. S. Ghosh, S. C. Bhattacharya and A. Saha, *Anal. Bioanal. Chem.,* 2010, **397,** 1573-1582.
8. S. Mondal, S. Ghosh, D. Ghosh and A. Saha, *J. Phys. Chem. C,* 2012**, 116,** 9774-9782.

9. E. G. Krebs, *in Methods in Enzymology* Vol. 1 (Colowick, S. P., and Kaplan, N. O., Eds.), Academic Press, New York, 1955, pp. 407-411.
10. R. M. Scheek and E. C. Slater, *Methods Enzymol.* 1982, **189**, 305-309.
11. F. Layne, *Methods Enzymol.,* 1957, **3**, 447-454.
12. I. H. Segel, Enzyme Kinetics: Behavior and analysis of rapid equilibrium and steady state kinetics, Wiley, New York, 1975.
13. M. Dixon, *Biochem. J.,* 1972**, 129**, 197-202.
14. J. I. Harris and M. Waters, in *The Enzymes* Vol. 13 (Boyer, P. D., ed.) 3rd Edn., (Academic Press), New York, 1976, pp. 1-49.
15. S. Bagui, M. Ray and S. Ray, *Eur. J. Biochem.*, 1999, **262**, 386-395.